Yang-Lee zeros, Julia sets, and their singularity spectra

Bambi Hu and Bin Lin
Department of Physics, University of Houston, Houston, Texas 77204-5504
(Received 14 October 1988)

We have studied the global scaling properties of the Julia sets of the Yang-Lee zeros of the s-state Potts model on the diamond hierarchical lattice. The singularity spectrum $f(\alpha)$ and the generalized dimension D_q are calculated for different s values. General observations are made on their variations.

I. INTRODUCTION

In recent years there has been much interest in the study of phase transitions on hierarchical lattices.[1] These lattices are iteratively constructed to be exactly self-similar. On the theoretical side, since the Migdal-Kadanoff renormalization group is exact, they provide a class of models about which precise statements can be made. On the practical side, since these models are highly inhomogeneous, they serve to give insights into the understanding of such physical systems as random magnets, polymers, percolation clusters, and superconducting networks.

On a hierarchical lattice, the exact renormalization-group recursion relation defines a rational mapping of the coupling constant. Associated with such a rational mapping in the complex plane is the Julia set. Recently a remarkable observation has been made[2] on the Julia set of the renormalization-group mapping. It has been shown that this Julia set is simply the limiting set of the Yang-Lee zeros of the partition function. Since the discovery of the famous Yang-Lee theorem,[3] very little is known about the distribution and structure of the zeros of the partition function, except for a few exactly solvable models. In the case of hierarchical lattices, fairly complete information about the Yang-Lee zeros has thus become available due to their connection to the Julia set.

In another line of development, it has been recognized that most of the fractals in nature are actually composed of an infinite set of interwoven subfractals, and hence the name "multifractal." To provide a more complete characterization of the global scaling properties of multifractals, one has to use a spectrum of critical exponents and their singularities.[4] Julia sets are multifractals. The singularity spectrum for the simplest quadratic complex mapping has been studied.[5] In view of the fact that the Julia sets associated with phase transitions on hierarchical lattices have physical meaning, it would be interesting to study their singularity spectra. However, unfortunately, it is still unclear what direct physical meaning one can attribute to the singularity spectrum of the Julia set of the Yang-Lee zeros.

In this paper we study the singularity spectrum of the Julia sets of the s-state Potts model on the diamond hierarchical lattice. In Sec. II the relation between the Yang-Lee zeros of the partition function and the Julia set of the renormalization-group recursion relation is reviewed. In Sec. III the thermodynamic formalism for the singularity spectrum is recapitulated. In Sec. IV the singularity spectra and the generalized dimensions of these Julia sets are presented and discussed. In Sec. V a summary of our results is given.

II. YANG-LEE ZEROS AND JULIA SETS

We will first review the beautiful work of Derrida *et al.*,[2] who have discovered the connection between the Yang-Lee zeros of the partition function and the Julia set of the renormalization transformation for the Potts model on hierarchical lattices.

The Hamiltonian of the s-state Potts model is

$$H=-J\sum_{\langle ij\rangle}\delta(\sigma_i,\sigma_j),\quad \sigma_i=1,2,\ldots,s \tag{1}$$

where δ is the Kronecker delta, and the sum is over nearest neighbors. The partition function is then given by

$$Z=\sum_{\{\sigma_i\}}\exp\left[K\sum_{\langle ij\rangle}\delta(\sigma_i,\sigma_j)\right], \tag{2}$$

where $K=\beta J$. For convenience, we use the variable $z=e^K$.

To derive the recursion relation for the partition function we first look at the first two levels of the construction, shown in Figs. 1(a) and 1(b). Summing over the trace, we easily obtain the following recursion relation:

$$A(z)Z_1(z')=Z_2(z), \tag{3}$$

where

$$A(z)=(2z+s-2)^2, \tag{4}$$

$$z'=f(z)=\left[\frac{z^2+s-1}{2z+s-2}\right]^2. \tag{5}$$

This transformation is simply the recursion relation obtained by using the Migdal-Kadanoff renormalization group, which is exact here. The general recursion relation between the partition function at the $(n-1)$th level and the nth level is

$$Z_n(z)=Z_{n-1}(z')[A(z)]^{4^{n-2}}. \tag{6}$$

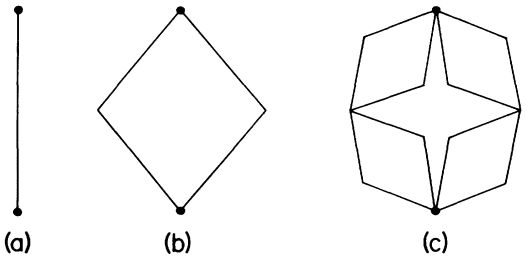

FIG. 1. Diamond hierarchical lattice.

There are 4^{n-1} bonds at the nth level; therefore, the partition function is a polynomial of degree 4^{n-1} in z. Let z_i be the zeros of $Z_n(z)$:

$$Z_n(z)=s\prod_{i=1}^{4^{n-1}}(z-z_i)\ . \tag{7}$$

Now one may rewrite Eq. (6) in the form of Eq. (7)

$$s\prod_{i=1}^{4^{n-1}}(z-z_i)=\left[s\prod_{i=1}^{4^{n-2}}(z'-z_i')\right](2z+s-2)^{2\times 4^{n-2}}\ , \tag{8}$$

where z_i' denotes the zeros of $Z_{n-1}(z)$. By using Eq. (5), Eq. (8) can be rewritten as follows:

$$\prod_{i=1}^{4^{n-1}}(z-z_i)=\prod_{i=1}^{4^{n-2}}[(z^2+s-1)^2-z_i'(2z+s-2)^2]\ . \tag{9}$$

Each factor on the right-hand side is a fourth-degree polynomial

$$P_i(z)=(z^2+s-1)^2-z_i'(2z+s-2)^2\ . \tag{10}$$

We notice that in Eq. (10) there is an equivalence between the zeros of $P_i(z)$ and the preimages of z_i' under the mapping f

$$P_i(z)=0\Longleftrightarrow z_i'=f(z)\ . \tag{11}$$

Therefore the four zeros of $P_i(z)$ are just the four preimages of z_i under the mapping f. This property allows one to obtain the 4^{n-1} zeros z_i of $Z_n(z)$ by working out the preimages of the 4^{n-2} zeros z_i' of $Z_{n-1}(z)$. Therefore, step by step, one can get the zeros of $Z_n(z)$ from the unique zero of $Z_1(z)=s(z+s-1)$, i.e., $z=1-s$. As $n\rightarrow\infty$, these preimages form exactly the Julia set of the transformation f in the complex z plane.[6]

The physical region of the set of zeros of the partition function $Z_n(z)$ is the positive real z axis. There will be no point in the set which lies on the positive real z axis if n is finite. As n increases some points will move toward the positive real z axis. Only when n is infinite will there be points reaching the physical region.

III. THERMODYNAMIC FORMALISM

In the thermodynamic formalism the partition function is defined by

$$\Gamma(q,\tau)=\sum_{i=1}^{N}\frac{p_i^q}{l_i^\tau}\ , \tag{12}$$

where l_i is the linear dimension of the ith piece and p_i its probability. In our case the probability is taken to be uniform for each piece. The function $\tau(q)$ can be determined from the implicit equation

$$\Gamma(q,\tau(q))=1\ . \tag{13}$$

Once $\tau(q)$ is obtained, the generalized dimension D_q and the exponent $\alpha(q)$ can be calculated:

$$D_q=\frac{\tau(q)}{q-1}\ , \tag{14}$$

$$\alpha(q)=\frac{d\tau(q)}{dq}\ . \tag{15}$$

The singularity spectrum $f(\alpha)$ is then given by the Legendre transformation

$$f(\alpha)=q\alpha(q)-\tau(q)\ . \tag{16}$$

In the limit $N\rightarrow\infty$, Eqs. (13)–(16) should give exact results; however, since in practice we can only deal with finite N, Eq. (13) gives very slow convergence. To improve the rate of convergence we will instead use the ratio method. Moreover, since we can only obtain $\tau(q)$ numerically, Eq. (15) is not very convenient. We will therefore derive an algebraic expression to calculate $\alpha(q)$.

Define the partition function at the nth level

$$\Gamma_n(q,\tau(q))=\sum_{i=1}^{N}\frac{p_i^q(n)}{l_i^\tau(n)}\ , \tag{17}$$

where $N=a^n$, a an integer. Then $\tau(q)$ can be determined from the equation

$$\frac{\Gamma_n(q,\tau(q))}{\Gamma_{n-1}(q,\tau(q))}=1\ , \tag{18}$$

i.e.,

$$\frac{\sum_{i=1}^{a^n}\left[\frac{p_i^q(n)}{l_i^\tau(n)}\right]}{\sum_{i=1}^{a^{n-1}}\left[\frac{p_i^q(n-1)}{l_i^\tau(n-1)}\right]}=1\ . \tag{19}$$

Here we have assumed that $\tau(q)$ is the same at level $n-1$ as level n. Because p_i is a constant we can express $q(\tau)$ explicitly. So we will use $q(\tau)$ instead of $\tau(q)$ to calculate $\alpha(q)$:

$$q(\tau)=\frac{\ln\left[\frac{\sum_i l_i^{-\tau}(n-1)}{\sum_i l_i^{-\tau}(n)}\right]}{-\ln\left[\frac{p(n-1)}{p(n)}\right]}\ , \tag{20}$$

$$\alpha(q(\tau)) = \frac{\ln\left[\frac{p(n-1)}{p(n)}\right]}{\frac{\sum_i l_i^{-\tau}(n-1)\ln l_i(n-1)}{\sum_i l_i^{-\tau}(n-1)} - \frac{\sum_i l_i^{-\tau}(n)\ln l_i(n)}{\sum_i l_i^{-\tau}(n)}} = \frac{\langle \ln p(n-1)\rangle - \langle \ln p(n)\rangle}{\langle \ln l(n-1)\rangle - \langle \ln l(n)\rangle} . \quad (21)$$

The average $\langle A(n)\rangle$ is weighed by $l_i^{-\tau}(n)/\sum_i l_i^{-\tau}(n)$. Equal probability means

$$p(n) = (Ia^n)^{-1} , \quad (22)$$

where I is an integer depending on the number of unstable fixed points. Substituting Eq. (22) into Eq. (21), one gets

$$\alpha(q) = \frac{\ln a}{\langle \ln l(n-1)\rangle - \langle \ln l(n)\rangle} . \quad (23)$$

Equation (16) is correspondingly changed to

$$f(\alpha) = q(\alpha)\alpha(q(\tau)) - \tau , \quad (24)$$

whereas Eq. (14) becomes

$$D_q = \frac{\tau}{[q(\tau)-1]} . \quad (25)$$

In the following, Eqs. (23)–(25) will be used to calculate $f(\alpha)$ and D_q.

In the case where the Julia set is one dimensional or quasi-one-dimensional, l_i is well defined.[4,5] But in our case the Julia sets are not quasi-one-dimensional. Figure 2 shows a typical Julia set of the Ising model ($s=2$) on the diamond hierarchical lattice. For such a Julia set the points are no longer well ordered. The usual way of defining l_i seems difficult to apply here. To overcome this difficulty we will instead use the method of derivatives.[6]

Consider a map f defined in the complex plane. We divide the set into N subsets, each subset containing only one point. We denote by $l(z_i)$ the size of the ith subset, i.e., $l(z_i)$ is the size of the piece containing the point z_i. Similarly, $l(z_{i-1})$ is the length for z_{i-1}, where z_{i-1} is the backward iterate of z_i: $z_{i-1}=f(z_i)$. The scaling function $\sigma(z_i)$ is defined by

$$\sigma(z_i) = \frac{l(z_i)}{l(z_{i-1})} , \quad (26a)$$

which can be approximated by

$$\sigma(z_i) = \frac{1}{|f'(z_i)|} . \quad (26b)$$

Since

$$l(z_i) = |f'(z_i)|^{-1} l(z_{i-1}) ,$$

continuing the backward iteration, one gets

$$\begin{aligned} l(z_i) &= |f'(z_i)|^{-1}|f'(z_{i-1})|^{-1}\cdots|f'(z_0)|^{-1} l_0 \\ &= |f'(z_i)|^{-1}|f'(f(z_i))|^{-1} \\ &\quad \times |f'(f^2(z_i))|^{-1}\cdots|f'(f^n(z_i))|^{-1} l_0 . \end{aligned} \quad (27a)$$

Backward iteration is a method that renders unstable fixed points stable. Here z_0 is the fixed point of $z_i, z_0 = f^n(z_i)$. l_0 is of order one, and therefore

$$l_i = |f'(z_i)f'(f(z_i))\cdots f'(z_0)|^{-1} . \quad (27b)$$

Equations (20)–(25) and (27) are the formulas we will use to calculate $f(\alpha)$ and D_q. To test the validity of this method, we have applied it to calculate $f(\alpha)$ and D_q for the maps $f(z)=z^n+c$ ($n>2$). The results are the same as those obtained by the direct method.

We briefly mention two limiting cases: $s\to 0$ and $s\to\infty$. As $s=0$, the rational recursion relation Eq. (5) degenerates into a polynomial of degree two,

$$f(z) = \tfrac{1}{4}(z+1)^2 . \quad (28)$$

The Julia set of this map is at the threshold of becoming a broken quasi-one-dimensional circle (Fig. 3). The two fixed points of the map coincide

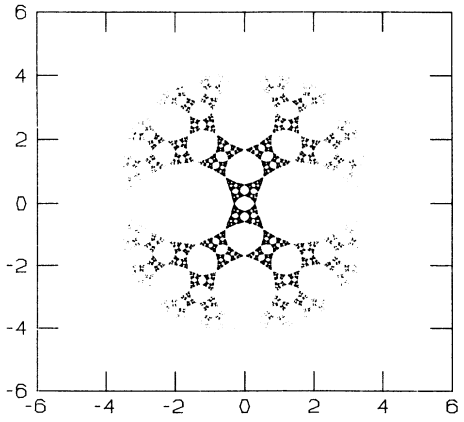

FIG. 2. Julia set for $s=2.0$ at level 6.

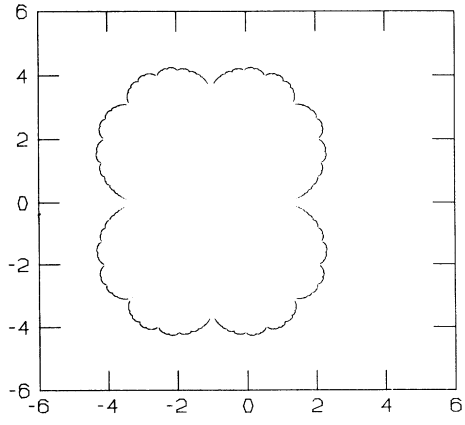

FIG. 3. Julia set for $s=0$ at level 6.

$$z_1^* = z_2^* = z^* = 1 \ . \tag{29}$$

This is the marginal case in which the circle is just about to break up. The Hausdorff dimension is equal to one. To perform a more careful analysis of the limiting behavior, let us examine Eq. (5) in detail. We found numerically that as $s \to 0$, $z_1^* \to 1^+$, $f'(z_1^*) \to 1$, $z_2^* \to 1^-$, $f'(z_2^*) \to \infty$, where z_1^* and z_2^* are the two unstable fixed points (see Table I). The extremal α values of the fixed points are determined by the derivatives at these points

$$\alpha = \frac{\ln p}{\ln |f'(z^*)|^{-1}} \ , \tag{30}$$

where p is now independent of n. Therefore

$$\alpha_{\max} = \frac{\ln p}{\ln |f'(z_1^*)|^{-1}} \to \infty \ , \tag{31}$$

$$\alpha_{\min} = \frac{\ln p}{\ln |f'(z_2^*)|^{-1}} \to 0 \ . \tag{32}$$

This agrees with the trend we have observed for $s = 1$ and 0.5, as shown in Fig. 4(a). Since $p \sim l^{\alpha}$, $\alpha \to \infty$ corresponds to $l_{\max} \to 1^-$, where the breaking points of the closed Julia set occur. And $\alpha \to 0$ corresponds to $l_{\min} \to 0$, the most concentrated parts of the Julia set. This infinite range of α indicates that the Julia set for $s \to 0$ is very nonuniform: $l_{\max}/l_{\min} \to \infty$. This behavior is quite different from that of $s \to \infty$, to be discussed below.

In the limit $s \to \infty$, the Julia set is unbounded, i.e., the invariant set is not distributed at a finite distance from the origin. Although we cannot get an analytic expression for the transformation, by examining the large s values, we can conjecture as to what the Julia set and

TABLE I. Fixed points and their derivatives for various s values.

s	Fixed points		Derivatives
0.5	0.162 434 564 7	0.000 000 000 0	0.330 068 031 3
	1.000 000 000 0	0.000 000 000 0	0.000 000 000 4
	0.730 405 563 6	0.000 000 000 0	138.267 583 171 6
	2.107 159 871 7	0.000 000 000 0	1.402 349 101 0
1.0	0.000 000 000 0	0.000 000 000 0	0.000 000 000 0
	1.000 000 000 0	0.000 000 000 0	0.000 000 000 0
	0.381 966 011 3	0.000 000 000 0	10.472 135 958 8
	2.618 033 988 8	0.000 000 000 0	1.527 864 045 0
1.5	−0.013 639 705 7	0.287 047 659 2	2.099 657 432 0
	1.000 000 000 0	0.000 000 000 0	0.000 000 000 0
	−0.013 639 705 7	−0.287 047 659 2	2.099 657 431 9
	3.027 279 411 3	0.000 000 000 0	1.613 023 065 1
2.0	−0.191 487 884 0	0.508 851 778 8	3.087 378 025 4
	1.000 000 000 0	0.000 000 000 0	0.000 000 000 0
	−0.191 487 884 0	−0.508 851 778 8	3.087 378 025 4
	3.382 975 767 9	0.000 000 000 0	1.678 573 510 4
2.5	−0.351 981 999 4	0.695 389 085 4	3.647 032 761 7
	1.000 000 000 0	0.000 000 000 0	0.000 000 000 0
	−0.351 981 999 4	−0.695 389 085 5	3.647 032 761 7
	3.703 963 998 8	0.000 000 000 0	1.732 220 386 3
3.0	−0.500 000 000 0	0.866 025 403 8	4.000 000 000 0
	1.000 000 000 0	0.000 000 000 0	0.000 000 000 0
	−0.500 000 000 0	−0.866 025 403 8	4.000 000 000 0
	4.000 000 000 0	0.000 000 000 0	1.777 777 777 8
3.5	−0.638 464 011 5	1.026 495 470 6	4.238 690 877 5
	1.000 000 000 0	0.000 000 000 0	0.000 000 000 0
	−0.638 464 011 5	−1.026 495 470 6	4.238 690 877 5
	4.276 928 023 1	0.000 000 000 0	1.817 441 381 4
4.0	−0.769 292 354 2	1.179 485 610 0	4.408 189 273 7
	1.000 000 000 0	0.000 000 000 0	0.000 000 000 0
	−0.769 292 354 2	−1.179 485 610 0	4.408 189 273 7
	4.538 584 708 5	0.000 000 000 0	1.852 601 595 8
4.5	−0.893 826 691 1	1.326 551 396 6	4.532 962 385 4
	1.000 000 000 0	0.000 000 000 0	0.000 000 000 0
	−0.893 826 691 1	−1.326 551 396 6	4.532 962 385 4
	4.787 653 382 2	0.000 000 000 0	1.884 199 154 4
5.0	−1.013 050 099 7	1.468 711 037 4	4.627 362 909 0
	1.000 000 000 0	0.000 000 000 0	0.000 000 000 0
	−1.013 050 099 7	−1.468 711 037 4	4.627 362 909 0
	5.026 100 199 4	0.000 000 000 0	1.912 902 460 1

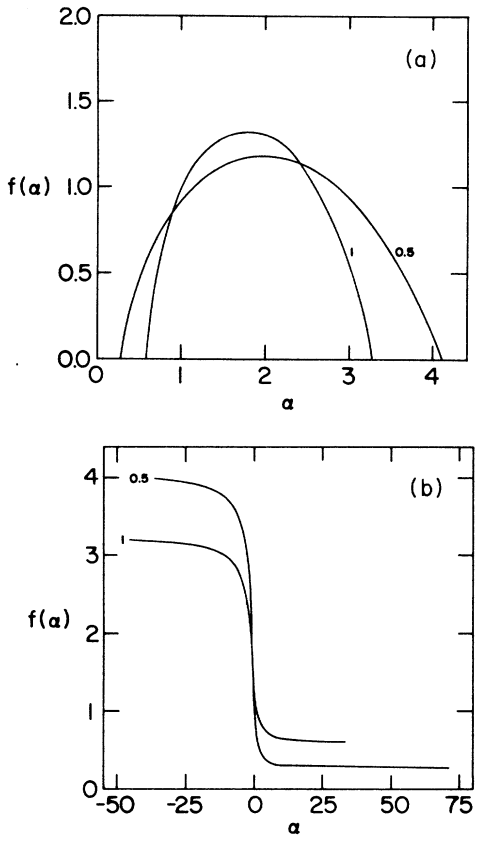

FIG. 4. $f(\alpha)$ and D_q for $s=0.5$ and 1.0 at levels 5 and 4. (a) $f(\alpha)$; (b) D_q.

$f(\alpha)$ look like as $s\to\infty$. In our numerical calculation, we found, for $s>s_1$, where $s_1=16$, the Julia set grows bigger, more uniform ($l_{\max}/l_{\min}\to 1$), and tends to a circle as s increases. At the same time $f(\alpha)$ becomes thinner and shorter, i.e., $\alpha_{\max}$, $\alpha_{\min}$, and $f_{\max}(\alpha)$ all approach one. We have examined this trend for $s=50-5000$. From those results, we conjecture that as $s\to\infty$, the Julia set is an infinite uniform circle, and $f(\alpha)$ is just one point: $f=\alpha=1$. Therefore the Julia set at $s\to\infty$ is no longer a multifractal, but simply a fractal like the uniform Cantor set.

IV. SINGULARITY SPECTRUM AND GENERALIZED DIMENSION

Since the complex rational map Eq. (5) is of power four, there are four fixed points given by the equation

$$z^*=\left[\frac{z^{*2}+s-1}{2z^*+s-2}\right]^2 . \tag{33}$$

It is easy to see that there is always a trivial fixed point for any s value: $z^*=1$. Excluding this trivial fixed point from Eq. (33), we get a cubic equation

$$z^3-3z^2+(3-2s)z-(s-1)^2=0 . \tag{34}$$

As observed by Itzykson and Luck,[2] Eq. (34) has three real roots corresponding to two unstable fixed points and one stable fixed point for

$$\frac{s^4}{4}-\frac{8s^3}{27}<0 , \tag{35}$$

i.e., $0<s<s_0$, where $s_0=\frac{32}{27}$. The significance of the stable fixed point was discussed in Refs. 2 and 7. If

$$\frac{s^4}{4}-\frac{8s^3}{27}>0 , \tag{36}$$

i.e., $s>s_0$ or $s<0$, there will be only one fixed point on the real axis, the other two fixed points being complex conjugates. Table I shows the fixed points and their derivatives for various s values. We see for $s>s_0$, there are three unstable fixed points, and only one is real, whereas for $s<s_0$, there are two unstable fixed points, both of which are real. As a consequence, the Julia sets, $f(\alpha)$ and D_q behave quite differently.

In Figs. 2, 3, 5, and 6 we have shown the Julia sets for some typical s values. For $s>s_0$, the Julia sets become denser as s decreases (Figs. 2 and 5); for $s<s_0$, it is just the opposite (Figs. 3 and 6). This feature is best reflected in the Hausdorff dimension. Figure 7 shows the Haus-

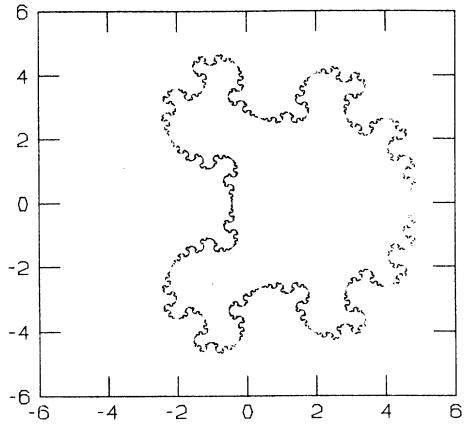

FIG. 5. Julia set for $s=4.5$ at level 6.

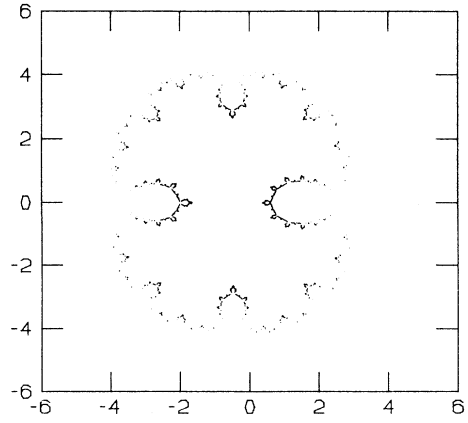

FIG. 6. Julia set for $s=1.0$ at level 6.

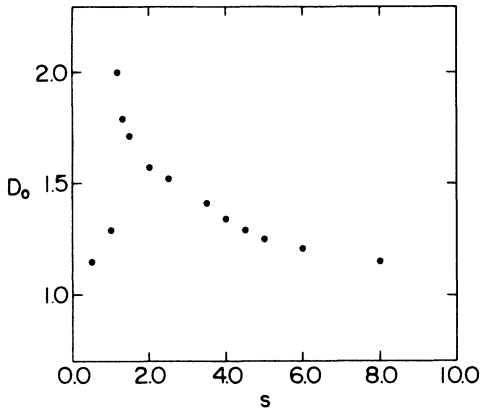

FIG. 7. Hausdorff dimension D_0 for the s-state Potts model. D_0 reaches its maximum value at $s=\frac{32}{27}$.

dorff dimension D_0 versus s. $D_0=1$ at $s=0$, it increases to its maximum value at $s=s_0$, then decreases again to its minimum value 1 as $s\to\infty$. Except for the limiting cases $s=0$ and $s\to\infty$, the Hausdorff dimensions of the Julia sets are all greater than one. This is expected because these Julia sets are not quasi-one-dimensional but planar. For $s>3$, there is only one point, $z_F>1$ on the positive real axis (Fig. 5). This corresponds to a ferromagnetic transition. For $s<3$, another point $0<z_A<1$ appears on the real axis with Fig. 2. This corresponds to an antiferromagnetic transition. Moreover, when $s<2^-$ additional points appear in the interval $0<z<1$ on the real axis (Fig. 6). We do not know if there is any physical significance that can be attributed to these points.

The singularity spectrum $f(\alpha)$ and the generalized dimension D_q are calculated for s between 0.5 and 5.0. For $s>s_0$, both $f(\alpha)$ and D_q change continuously with s. As s decreases, the $f(\alpha)$ curve moves to the right and becomes higher [Figs. 8(a) and 9(a)] while D_q moves up [Figs. 8(b) and 9(b)]. However, as s passes through s_0, this trend ceases. Figure 4(a) shows $f(\alpha)$ for $s=1.0$ and 0.5. It is shorter and bigger than that for $s=1.5$. Correspondingly, D_q becomes a higher kink [Fig. 4(b)]. For $s<s_0$, as s decreases, $f(\alpha)$ becomes shorter and stretches along the real axis [Fig. 4(a)]. D_q at the same time becomes a higher kink. Eventually when $s\to 0$, $f(\alpha)$ will extend to the whole semi-infinite real axis, i.e., $\alpha_{\min}\to 0$, $\alpha_{\max}\to\infty$, and D_q will be an infinitely high kink.

For $s>s_0$, $f(\alpha)$ and D_q also differ for $s>3$ and $s<3$. When $s>3$, among the three repelling fixed points, the point of the type $(a,0)$ is located at the most rarefied point (corresponding to $\alpha_{\max}$), whereas the other two conjugate points of type (a,b) and $(a,-b)$ are located at the most concentrated points (corresponding to $\alpha_{\min}$). Because of these special fixed points the $f(\alpha)$ curves, no matter how low the level of calculation is, have exact $\alpha_{\min}$ and $\alpha_{\max}$. Therefore the $f(\alpha)$ and D_q curves converge very quickly. Figure 10 shows the $f(\alpha)$ curves for $s=4.5$ at levels 5 and 4, respectively. We see that they almost coincide even at these low levels. But as we go below $s=3$, none of these repelling fixed points correspond to $\alpha_{\min}$ or $\alpha_{\max}$, and the rate of convergence for both $f(\alpha)$

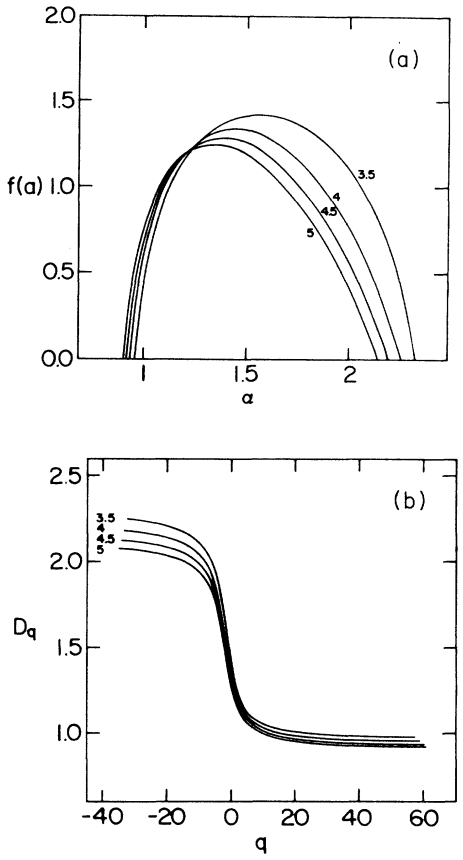

FIG. 8. Singularity spectra $f(\alpha)$ and generalized dimensions D_q for $s=3.5$, 4, 4.5, and 5, all at levels 4. (a) $f(\alpha)$; (b) D_q.

and D_q becomes very slow and irregular. Figure 11 shows $f(\alpha)$ for $s=1.5$ at levels 7 and 6. Compared with the $f(\alpha)$ curves for $s=4.5$ shown in Fig. 10, we see that even at these higher levels the convergence of $f(\alpha)$ for $s=1.5$ is much worse than that for $s=4.5$. The gap between $f_{\min}$ and 0 in Fig. 11 indicates that one needs to go to higher levels to obtain better convergence.

We should also like to mention the difficulties we encountered when we tried to calculate $f(\alpha)$ and D_q for $s=3$. There are lots of $l_i>1$ which are not allowed because they will give probabilities greater than one. The left side of $f(\alpha)$ converges well, but the right side does not converge even at very high levels. This may serve as a hint that the derivative method may not be universally applicable. Let us see in more detail what happens when $s=3$. From Eq. 27(b), $f'(z)$ can be obtained from the renormalization transformation equation (5)

$$f'(z)=\frac{4(z-1)(z+s-1)(z^2+s-1)}{(2z+s-2)^3}\ . \tag{37}$$

If in a Julia set there are some points z_i which make $f'(z_i)$ less than one, there will be lots of $l_i>1$ including not only those badly located points but also some of their preimages. The higher the level, the more irregular lengths there are. In the Julia set for $s=3$ we can see that there are some points (at a finite level) very close to

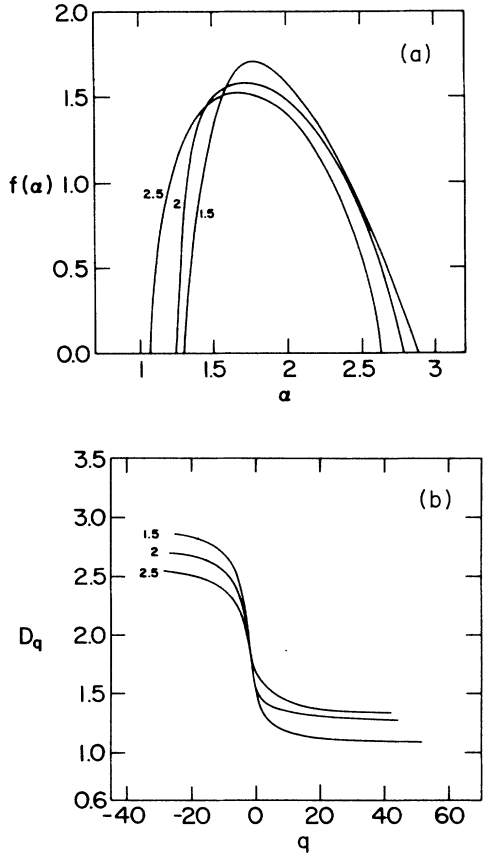

FIG. 9. $f(\alpha)$ and D_q for $s=1.5$, 2.0, and 2.5 at levels 7, 6, and 5, respectively. (a) $f(\alpha)$; (b) D_q.

the dangerous points $\bar{z}_1=-2$, $\bar{z}_{2,3}=\pm i\sqrt{2}$. From Eq. (37) one notes that these are the points at which the derivative vanishes. Re-expressing Eq. (23), we can show

$$\alpha=\frac{\ln a}{\dfrac{\sum_i l_i^{-\tau}(n-1)\ln l_i(n-1)}{\sum_i l_i^{-\tau}(n-1)}-\dfrac{\sum_i l_i^{-\tau}(n)\ln l_i(n)}{\sum_i l_i^{-\tau}(n)}} .$$

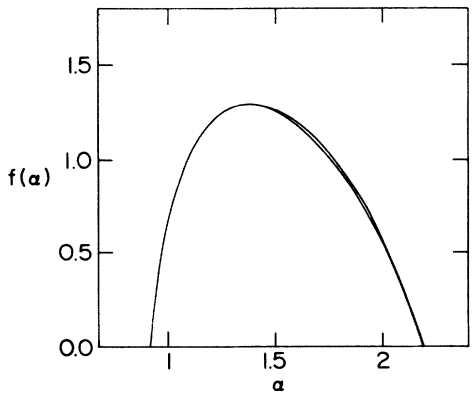

FIG. 10. $f(\alpha)$ for $s=4.5$ at levels 5 and 4, respectively.

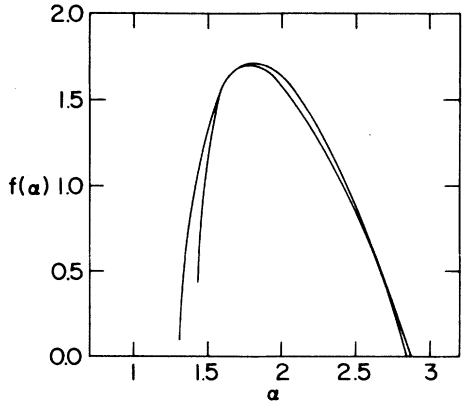

FIG. 11. $f(\alpha)$ for $s=1.5$ at levels 7 and 6, respectively.

As $\tau\to-\infty$, the dominant terms in both terms in the denominator are $l_{\max}(n-1)$ and $l_{\max}(n)$, respectively. At a given level n

$$\alpha_{\max}=\frac{\ln a}{\ln l_{\max}(n-1)-\ln l_{\max}(n)}=\frac{\ln a}{\ln\left[\dfrac{l_{\max}(n-1)}{l_{\max}(n)}\right]} , \tag{38}$$

$$\alpha_{\min}=\frac{\ln a}{\ln\left[\dfrac{l_{\min}(n-1)}{l_{\min}(n)}\right]} . \tag{39}$$

Now it is clear why the left side of $f(\alpha)$ for $s=3$ converges but the right side does not. $\alpha_{\min}$ is determined by $l_{\min}$, i.e., $\max|f_i'f_{i-1}'\cdots f_0'|$; therefore, it is not affected by the points around $\bar{z}_i$. $\alpha_{\max}$, on the other hand, is determined by $l_{\max}$, i.e., $\min|f'f'\cdots f'|$. The points with derivatives less than one will make $l_{\max}(n-1)/l_{\max}(n)$ very unstable.

V. SUMMARY

In this paper we have studied the global scaling properties of the Julia sets of the Yang-Lee zeros of the s-state Potts model on the diamond hierarchical lattice. The singularity spectrum $f(\alpha)$ and the generalized dimension D_q are calculated for various s values. Due to the difference in behavior of $f(\alpha)$ and D_q, we divided s into three groups: $s<s_0$, $s_0<s<s_1$, and $s>s_1$, where $s_0=\frac{32}{27}$ and $s_1=16$. For $s>3$, there is only a ferromagnetic transition point; for $s<3$, another antiferromagnetic transition point appears. Moreover, for $s<2^-$, there are additional points that appear on the positive real axis. We are, however, unsure about the physical significance of these additional points. The most important remaining question is, of course, what direct physical meaning one can attribute to the singularity spectrum of the Julia set of the Yang-Lee zeros. Unfortunately at present we have no good answer to this question. We, however, hope this question can be answered in the future.

ACKNOWLEDGMENTS

We would like to thank P. Cvitanovic and M. H. Jensen for stimulating and valuable discussions. Correspondence with J. M. Luck was also appreciated. This work was supported in part by the Texas Center for Superconductivity.

[1]A. N. Berker and S. Ostlund, J. Phys. C **12**, 4961 (1979); R. B. Griffiths and M. Kaufman, Phys. Rev. B **26**, 5022 (1982), and references therein.

[2]B. Derrida, L. De Seze, and C. Itzykson, J. Stat. Phys. **33**, 559 (1983); B. Derrida, C. Itzykson, and J. M. Luck, Commun. Math. Phys. **94**, 115 (1984); C. Itzykson and J. M. Luck, *Progress in Physics* (Birkhauser, Basel, 1985), Vol. 11, p. 45.

[3]C. N. Yang and T. D. Lee, Phys. Rev. **87**, 404 (1952); T. D. Lee and C. N. Yang, *ibid.* **87**, 410 (1952).

[4]T. C. Halsey, M. H. Jensen, L. P. Kadanoff, I. Procaccia, and B. I. Shraiman, Phys. Rev. A **33**, 1141 (1986).

[5]M. H. Jensen, L. P. Kadanoff, and I. Procaccia, Phys. Rev. A **36**, 1409 (1987).

[6]T. Bohr, P. Cvitanovic, and M. H. Jensen, Europhys. Lett. (to be published).

[7]A. N. Berker and L. P. Kadanoff, J. Phys. A **13**, L259 (1980).